Vortex Panel Calculation of Wake Rollup Behind a Large Aspect Ratio Wing

D.T. Yeh*
Stanford University, Stanford, California
and
A. Plotkin†
San Diego State University, San Diego, California

A higher-order (linear vortex) panel method is used to calculate the three-dimensional wake rollup behind large aspect ratio symmetric wings in steady inviscid incompressible flow. Triangular-shaped panels are chosen to increase the geometric flexibility of the wake sheet. The wing spanwise circulation distribution is obtained from lifting-line theory, and the wake geometry is then evaluated in an iterative fashion by satisfying conservation of circulation, flow tangency, and zero-pressure jump for all wake panel surfaces in the near-wake region (two spans in length). The far wake is modeled by straight semi-infinite vortex filaments that are in the uniform stream direction. Numerical results are shown to compare favorably with those in the literature. The capability of the method to model a rectangular wing with a deflected flap is also studied.

Introduction

Background

THE accurate calculation of the position and strength of the vortex wake behind a blade in motion is a critical problem for rotorcraft applications. A detailed model of the vortex wake would permit substantial improvements in many aspects of rotary wing design such as performance, acoustics, vibrations, and response. For the vortex flow behind a wing of finite span at angle of attack, there exists a pressure differential between the top and bottom surfaces as a byproduct of the lift force. The vorticity is shed as a result of the difference in the direction of the flow between the wing surfaces at the trailing edge.

For high Reynolds number flow past a thin wing at moderate angles of attack, convection dominates diffusion and the vorticity is confined to a thin, free shear layer. Under the influence of the self-induced velocity, the shear layer has the tendency to roll up into vortex cores. In the downstream direction, the vorticity is continuously fed into the vortex cores resulting in a growth both in strength and dimension. Further downstream of the wing, the rollup process will be completed and most of the vorticity is contained within the cores. At this stage, the velocity gradients in the cores are large and the viscous effects become important. Consequently, instabilities may occur which can result in the breakup of the trailing vortex system. The present research only considers the initial stage of the wake rollup—potential flow is considered with embedded vortex sheets.

Received May 27, 1985; presented as Paper 85-1561 at the AIAA Fluid Dynamics, Plasmadynamics and Lasers Conference, Cincinnati, OH, July 16-18, 1985; revision received Dec. 15, 1985. Copyright © American Institute of Aeronautics and Astronautics, Inc., 1986. All rights reserved.

*Graduate Student, Department of Aeronautics and Astronautics; formerly, Student, Department of Aerospace Engineering, University of Maryland, College Park. Student Member AIAA.

†Professor and Chairman, Department of Aerospace Engineering and Engineering Mechanics; formerly, Professor of Aerospace Engineering, University of Maryland, College Park. Associate Fellow AIAA.

An excellent review of the literature on vortex wakes is given by Hoeijmakers.[1] Many of the studies use a two-dimensional time-dependent analogy to study the wake rollup for the large aspect ratio case. The technique is developed under the assumptions that the flow varies slowly in the streamwise direction and that there is no direct influence due to the upstream wing. The two-dimensional time-dependent problem can be considered as a marching problem in the sense that the vortex sheet is determined at each cross-flow (Trefftz) plane and is convected with its own induced velocity in subsequent cross-flow planes. There have been many methods developed to model the vortex sheet motion using this analogy. The work by Fink and Soh[2] appears to be the most successful in producing smooth wake rollup by using the discrete-vortex method. Murman and Stremel[3] utilized the "cloud-in-cell" method to capture the vortex wake motion. A sophisticated second-order doublet panel method (curved segments) developed at the National Aerospace Laboratory (NLR), the Netherlands,[4] is capable of describing complicated vortex sheet motion, and vortex cores are also included to model highly rolled up regions.

Through the advance of computer technology, a number of fully three-dimensional flow models have been developed for the prediction of the wake rollup. The vortex-lattice method has found wide application for computing the attached-flow loading of lifting surfaces. In the vortex-lattice method the lifting surface is divided into elements. Each element carries a line vortex along its quarter-chord line connected to line vortices trailing to infinity downstream along the side edges of the element. The strengths of the vortices are determined by imposing the no-penetration condition at the midpoint of the quarter-chord line of the elements. Rom and Zorea[5] developed a computational procedure to relax the wake. They use a finite number of line vortices to represent the trailing vortex sheet. The wake geometry is evaluated in an iterative fashion starting from an assumed initial wake position. Suciu and Morino[6] developed a method that uses constant doublet panels on the wing and wake to calculate the wake rollup behind rectangular wings. The use of constant doublet panels for the wake modeling is equivalent to using vortex filaments. In recent years, the constant doublet panel method has been widely applied to helicopter applications to model the blade and wake.[7,8]

For cases when the vortex wake passes close to a lifting surface, the filament wake model may not be adequate to describe the flow details. This is true for the leading-edge sheet of a low aspect ratio wing.[1] It is also noted that a higher-order panel method solution for the wake rollup behind a large aspect ratio wing is not available in the literature.

Higher-order panel methods for three-dimensional vortex calculations have been developed by Johnson et al.,[9] Hoeijmakers and co-workers (see Ref. 1), and Kandil et al.[10,11] These methods have been used to study leading- and side-edge separation for low aspect ratio wings. The methods developed at Boeing[9] and NLR[1] use second-order doublet distributions.

In the method of Kandil et al.,[10,11] vortex panels (triangular panels in the wake) with a first-order vorticity distribution are used in the near-field calculations. In the far-field calculations, the distributed vorticity over each far-field panel is lumped into equivalent concentrated vortex lines. We choose to modify this vortex panel method and apply it to large aspect ratio wings with a closer look at the trailing wake rollup.

It is the purpose of the present research to consider a higher-order (linear vortex) panel method for the vortex wake modeling. The technique is first developed for a finite wing in steady flight as the initial step toward the helicopter free-wake analysis.

Approach

A theoretical investigation is made to calculate the three-dimensional wake geometry in a steady incompressible flow behind a symmetrical wing of large aspect ratio ($\mathcal{R}$) for a given spanwise circulation distribution (obtained from lifting-line theory). This method uses triangular vortex panels with a linear vorticity distribution for near-wake modeling. To model this problem, the wake is first initialized as a flat sheet of zero thickness, extending from the wing trailing edge (TE), which is divided into three regions—adjoining, near, and far regions, as shown in Fig. 1.

The adjoining region is described as a small region of planar vortex sheet where the wake surface lies in the direction of the chord axis and stays fixed. This region is introduced to model the satisfaction of the Kutta condition that the flow will leave the trailing edge smoothly.

In the near region, approximately two spans in length, the wake surface is split into a network of flat, triangular elements (panels) with linearly distributed vorticity in the local spanwise direction and constant vorticity along the streamwise direction (local flow direction).

In the far region, straight semi-infinite vortex filaments of equivalent strengths are shed from the TE of the vortex panel sheet to infinity. Such representation for the far wake is introduced for economic feasibility while accuracy is maintained in the near region as well.

The wake geometry is then evaluated in an iterative fashion by satisfying conservation of circulation, the flow tangency condition, and zero-pressure jump for all wake panel surfaces in the near region. The iteration continues until the wake shape converges, or equivalently, the wake sheet truly becomes a stream surface in the near region. Straight semi-infinite vortex filaments in the far wake are assumed to be in the uniform stream direction.

The flow problem of a wing-flap configuration is also studied by utilizing the current wake model. This is studied to demonstrate the versatility of the present model as well as the effect of a flap on the wake rollup of a rectangular wing.

Mathematical Problem

Consider the flow of a steady freestream of speed U_∞ at angle of attack α past a thin wing of large $\mathcal{R}$, as shown in Fig. 1. Since the flowfield considered here is the high Reynolds number flow past a thin wing at a moderate angle of attack, the viscous boundary layer and wake are essentially confined to a thin region. Outside the boundary layer and wake, the velocity gradients become so small that the shear stresses acting on a fluid element are negligible. For a region near the center of the rolled up region, however, velocity gradients are large and the viscous effects become dominant.[1] In the present study only the initial rollup stage is analyzed and, consequently, the fluid is considered to be inviscid.

The global reference frame is expressed in terms of a space-fixed Cartesian coordinate system (x,y,z), where the x axis is in the direction of the freestream velocity, the y axis is in the spanwise direction, and the z axis is perpendicular to the x and y axes such that a right-handed coordinate system is formed. The midpoint on the wing TE (or lifting line) serves as the origin.

The freestream velocity vector can be expressed as

$$U_\infty = U_\infty \boldsymbol{i} \tag{1}$$

The continuity equation for an incompressible flow is

$$\nabla \cdot \boldsymbol{V} = 0 \tag{2}$$

and the flow irrotationality condition is

$$\nabla \times \boldsymbol{V} = 0 \tag{3}$$

where $\boldsymbol{V}$ is the velocity vector. Equation (3) holds everywhere in the flowfield except on the wake surface and on the lifting line, where the rotational regions are confined. If we define the velocity potential Φ and perturbation velocity potential ϕ such that

$$\boldsymbol{V} = U_\infty \boldsymbol{i} + \nabla\phi = \nabla\Phi \tag{4}$$

then Eq. (3) is satisfied identically.

Substituting Eq. (4) into Eq. (2), the Laplace equation for both Φ and ϕ is obtained. The no-penetration condition is applied to enforce flow tangency on the wake surface,

$$(U_\infty \boldsymbol{i} + \nabla\phi) \cdot \nabla W = 0 \qquad \text{on } W(x,y,z) = 0 \tag{5}$$

where $W(x,y,z) = 0$ is the equation of the wake surface.

The zero-pressure jump condition is given in Ref. 11 as

$$0 = \Delta C_p = 2(\boldsymbol{n}_w \times \boldsymbol{\omega}) \cdot \boldsymbol{V}/U_\infty^2 \qquad \text{on } W(x,y,z) = 0 \tag{6}$$

where $\boldsymbol{n}_w$ is the unit vector normal to the sheet and $\boldsymbol{\omega}$ is the vorticity vector.

Since Eq. (5) requires the velocity to be tangent to the wake surface, Eq. (6) implies that the vorticity is parallel to the local velocity in order to have zero-pressure jump on the sheet.

In addition, the velocity must approach the freestream value as the distance from the wake surface becomes large,

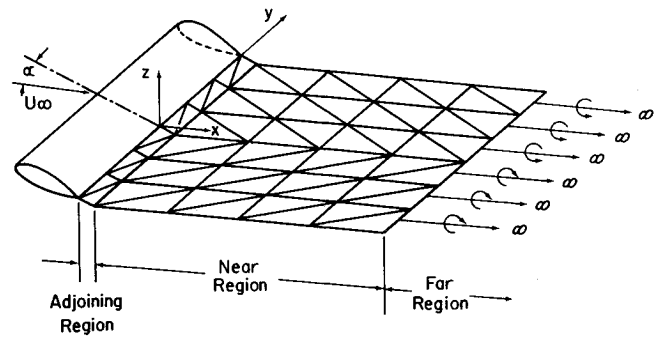

Fig. 1 Initial wake geometry.

which leads to the infinity condition

$$\nabla\phi \to 0 \text{ as } \sqrt{x^2+y^2+z^2} \to \infty \text{ and away from } W \quad (7)$$

From Kelvin's theorem for an inviscid flow,

$$\frac{D\Gamma}{Dt}=0 \quad (8)$$

Physically, it states that once the circulation around a fluid curve is generated, its strength remains constant as the same fluid particles are convected downstream.

Method of Analysis

This section introduces the numerical formulation and basic elements involved in the present higher-order panel method, including wing modeling, treatment of the wake, and, ultimately, the wake rollup iteration procedure.

The emphasis in this study is on the calculation of the wake rollup. For the large aspect ratio case considered here, Suciu and Morino[6] demonstrated that the effect of the wake rollup on wing loading was negligible. Therefore, for simplicity, the spanwise circulation distribution is calculated with the use of Prandtl's lifting-line theory (see, for example, Karamcheti[12]) and is not updated during the wake rollup iteration. (The rollup procedure developed here can be used in conjunction with any wing loading calculation method which supplies the spanwise circulation distribution.)

Once the spanwise circulation distribution $\Gamma(y)$ is obtained from the lifting-line theory, the vorticity shed by the wing (or the strength of the trailing vortex sheet) can be expressed as

$$\omega=-\frac{d\Gamma}{dy} \quad (9)$$

The direction of the shed vorticity is taken to be perpendicular to the lifting line.

For a piecewise linear distribution of vorticity in the spanwise direction, along with the fact that the change of circulation ($\Gamma_i-\Gamma_{i+1}$) must be shed behind and into the wake (Fig. 2), Eq. (9) can be written as follows with the use of the trapezoidal rule:

$$(\omega_i^n+\omega_{i+1}^n)\left[\frac{y_{i+1}^n-y_i^n}{2}\right]=-(\Gamma_{i+1}-\Gamma_i)=\text{const} \quad (10)$$

where the superscript n denotes the nth row of panels downstream.

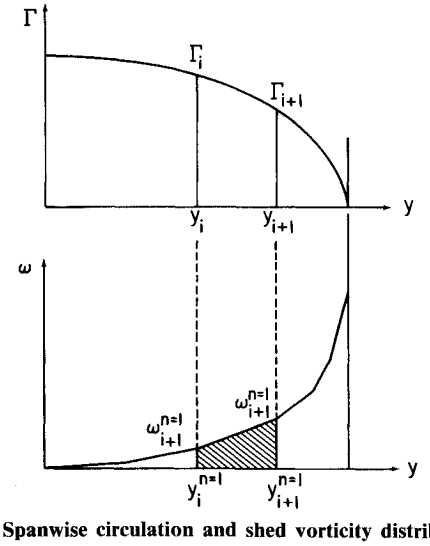

Fig. 2 Spanwise circulation and shed vorticity distribution.

As a consequence of Kelvin's circulation theorem, the circulation around a closed curve bounded by streamlines remains constant for all times. Referring to Fig. 2, Eq. (10) reflects that the vorticity distribution is adjusted such that the shaded area under the vorticity curve is always equal to the change of the circulation provided that the vorticity is continuous at the common node between two adjacent panels. By using Eq. (10) for ω_{i+1}^n along with the symmetry condition

$$\omega_{i=1}\,|_{y=0}\equiv 0 \quad (11)$$

the value of vorticity at each nodal point can be obtained starting from the symmetry plane and marching outward.

Equation (6) requires the vorticity on the wake to be parallel to the flow, while the local $\bar{x}$ axis is designated as the local stream direction (see Fig. 3). Therefore, the vorticity vector is given as

$$\omega=\omega e_x \quad (12)$$

where e_x is the unit vector in the local $\bar{x}$ direction. (Note that this assumes the velocity to be in the same direction across a panel, an approximation that improves as the number of panels increases.) Furthermore, vorticity is divergence-free,

$$\nabla\cdot\omega=0 \quad (13)$$

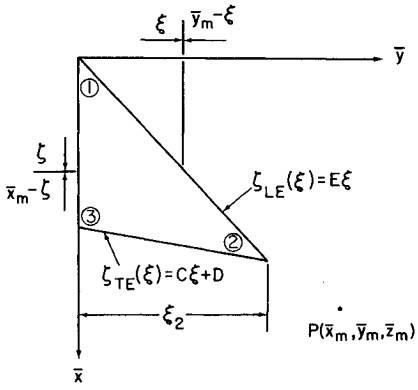

Fig. 3 Geometry of a triangular panel.

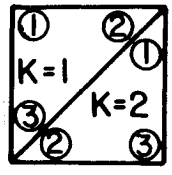

Fig. 4a Local panel numbering system.

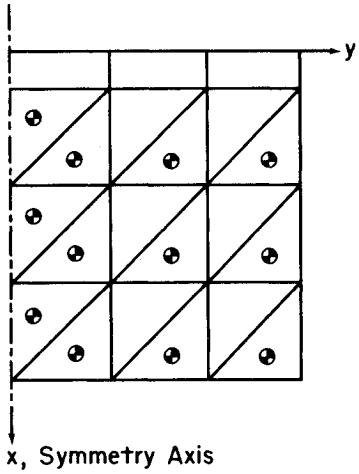

Fig. 4b Locations of the control points.

since $\nabla \cdot (\nabla \times V) = 0$.

Substituting Eq. (12) into Eq. (13) yields

$$\frac{\partial \omega}{\partial \bar{x}} = 0 \tag{14}$$

Equation (14) shows that the vorticity distribution on each panel is independent of $\bar{x}$, or the vorticity remains constant along the streamwise direction for each panel.

Induced Velocity

The induced velocity at a point on the wake surface is calculated by summing the contributions from three major sources. They are:

1) Bound vortex segments for the wing modeling.

2) Triangular vortex panels in the adjoining and near regions.

3) Straight semi-infinite vortex filaments in the far region.

Straight Vortex Segments

The lifting-line model is used to take account of the presence of a three-dimensional wing, where a series of bound vortex segments is placed along the lifting line. Cosine spacing is used to divide the lifting line into segments, with the emphasis on the wingtip region where the circulation distribution is expected to change rapidly. Moreover, to increase the accuracy of the influence of the lifting line, each segment is further divided into two equal-length subsegments with locally piecewise linear distribution of circulation.

Once the continuous vortex sheet ends in the near region, the far-wake representation is carried out by straight semi-infinite vortex filaments of equivalent strengths. These filaments are shed from the midpoints of the TE panels to infinity with the direction of the freestream velocity. The strength of each filament is determined from the change of the circulation distribution at the corresponding wing section upstream, and remains constant throughout the far region.

The Biot-Savart law is used to calculate the velocity induced by both the lifting line and the far wake.

Triangular Vortex Panels

The velocity induced by a distribution of vorticity on the surface σ at the field point $P(\bar{x}_m, \bar{y}_m, \bar{z}_m)$ in the local panel coordinates can be calculated by means of the Biot-Savart law to yield

$$\bar{V}(\bar{x}_m, \bar{y}_m, \bar{z}_m) = -\frac{1}{4\pi} \int_\sigma \int \frac{(r-s) \times \omega}{|r-s|^3} d\sigma \tag{15}$$

where $r = \bar{x}_m e_x + \bar{y}_m e_y + \bar{z}_m e_z$ is the position vector of point P, and $s = \zeta e_x + \xi e_y$ is the position vector of a point in σ.

On the vortex panel, a local linear distribution of vorticity is considered along the local spanwise direction, which can be expressed as

$$\omega = (A + B\xi) e_x \tag{16}$$

where A and B are obtained by satisfying the spatial conservation of circulation, and ξ is the distance in the $\bar{y}$ direction measured from the local origin.

Carrying out the cross product and using the definition of the panel geometry as shown in Fig. 3, Eq. (15) becomes

$$\bar{V}(\bar{x}_m, \bar{y}_m, \bar{z}_m) = -\frac{1}{4\pi} \int_0^{\xi_2} \int_{\zeta_{LE}(\xi)}^{\zeta_{TE}(\xi)} \frac{(A + B\xi)[\bar{z}_m e_y - (\bar{y}_m - \xi) e_z]}{[(\bar{x}_m - \zeta)^2 + (\bar{y}_m - \xi)^2 + \bar{z}_m^2]^{3/2}} d\zeta d\xi \tag{17}$$

This integral can be evaluated in closed form (the details can be found in Ref. 13).

Control Points

The control points are introduced here as the points at which the resultant flow is required to be tangent to the panel surfaces. The control point is chosen to be the geometric center of a triangular panel, which is defined as the intersection of the lines drawn from the vertices that bisect their opposite sides.

Moving the Panels

In the present study, each of the triangular panels is considered to be a stream surface composed of the streamlines that are parallel to one another with respect to the side 1-3 (see Fig. 3). Once the induced velocity at a control point is determined, the streamline which contains the control point is moved in the same direction as that of the local velocity.

To demonstrate the approach, the unit vector of the streamline at the control point e_{cp} is given by

$$e_{cp} = \frac{\bar{u}_R}{\bar{V}_R} e_x + \frac{\bar{v}_R}{\bar{V}_R} e_y + \frac{\bar{w}_R}{\bar{V}_R} e_z \tag{18}$$

where $\bar{u}_R$, $\bar{v}_R$, and $\bar{w}_R$ are the components of the induced velocity in the $\bar{x}$, $\bar{y}$, and $\bar{z}$ directions, respectively, and $\bar{V}_R = (\bar{u}_R^2 + \bar{v}_R^2 + \bar{w}_R^2)^{1/2}$. Side 1-3 is then moved in the direction parallel to the unit vector and, with the use of Eq. (18),

$$l_{13} = |l_{13}| \left(\frac{\bar{u}_R}{\bar{V}_R} e_x + \frac{\bar{v}_R}{\bar{V}_R} e_y + \frac{\bar{w}_R}{\bar{V}_R} e_z \right) \tag{19}$$

where $l_{13} = \bar{x}_3 e_x + \bar{y}_3 e_y + \bar{z}_3 e_z$ is the position vector of point 3 in the local coordinates (recall that point 1 is the local origin), and $|l_{13}|$ is the length of side 1-3 and remains constant throughout the computation.

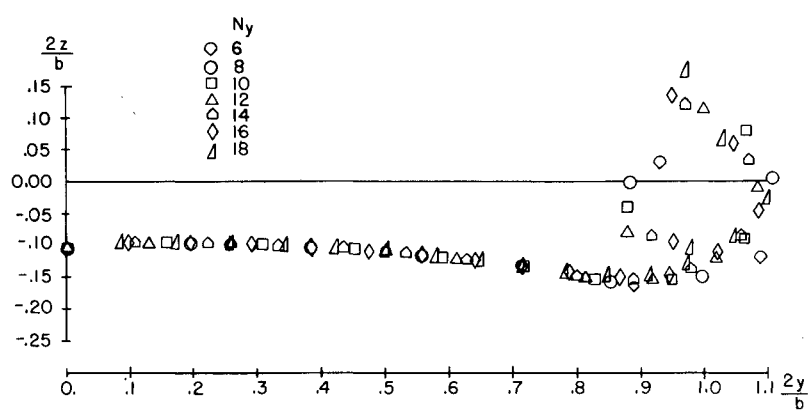

Fig. 5 Convergence study for a rectangular wing: $AR = 8$; $\alpha = 5$ deg; $x_w/b = 1.69$.

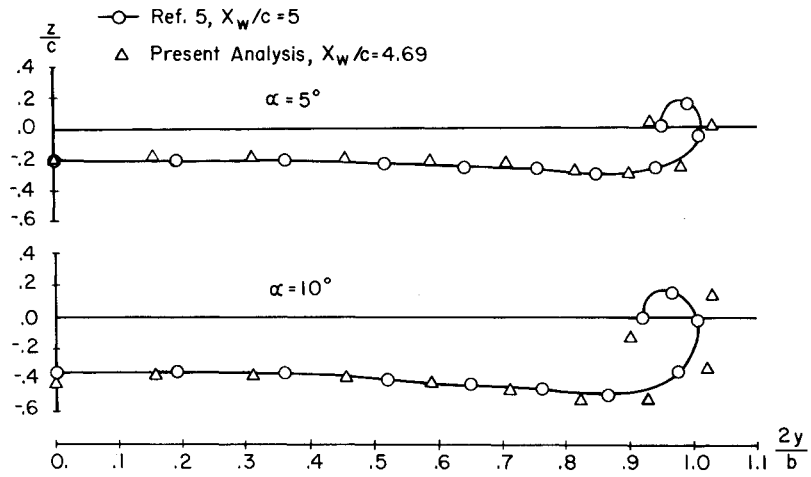

Fig. 6 Wake shapes at different angles of attack for a rectangular wing: $\mathcal{R} = 8$.

Because the number of triangular panels is always greater than the number of corner points, Fig. 4 shows that only the control points on the $K = 2$ panels are used to move the nodes such that side 1-3 of each triangular panel is aligned in the direction of the streamlines. The nodal points along the centerline, however, are moved according to the control points of the $K = 1$ panels along the symmetry line.

Wake Rollup Iteration Procedure

This section presents the wake rollup iteration procedure which is an extension of the previous discussion that illustrates the mechanism to move a single panel surface. The objective of the iteration is to satisfy the boundary conditions on the panel surfaces; at the same time, the panel surfaces have to be connected so that a continuous wake sheet is formed.

To develop an efficient computational technique, an idea similar to overrelaxation is adopted in the first iteration such that a newly adjusted or better extrapolated downstream wake shape is introduced whenever a row of upstream panels is moved. The numerical procedure for the first iteration is summarized as follows:

1) The first row of panels lies in the direction of the chord axis and stays fixed.

2) The computation is initiated by specifying the rest of the wake to be planar (in the x direction).

3) Align the second row of panels with the local velocities.

4) The downstream wake shape is adjusted so that the nodal points will have the same y and z coordinates as that of the second row. The vorticity distribution is calculated again due to the new wake geometry.

5) Align the third row of panels with the local velocities, and adjust the downstream wake shape in the same way as in step 4.

6) This process continues until the last row of panels is moved in the direction of the local velocity.

Starting from the second iteration, the procedure is altered due to the fact that the geometry of the upstream wake will be affected by the change of the wake shape downstream which is left out in the first iteration. To continue the iteration, the following steps are used.

1) Calculate the resultant velocities at all of the control points.

2) Move the downstream nodal points simultaneously in the directions of the local velocities and connect these points to form the new wake sheet.

3) Adjust the vorticity distribution to account for the change of the wake geometry.

4) Repeat steps 1-3 until the wake shape is converged, or the change of the successive wake geometries becomes sufficiently small (i.e., Δy and Δz are less than 0.0005 of span length at each node).

Results and Discussion

The method of calculating the wake shape behind a symmetric wing is implemented using a computer program. In the program, the initial wake geometry is automatically generated by dividing the straight wake into Nx rows and Ny columns (semispan) to form $(Nx)(Ny)$ rectangular elements. Each rectangular element is then divided into two triangular panels.

In the wake rollup calculations, the panels in the near wake are distributed using cosine spacing in the spanwise and streamwise directions to emphasize the details near the wingtip and lifting line, respectively. For all of the numerical runs presented, the results of the wake shapes are shown only for the half-plane from the symmetry axis.

The convergence properties of the method are studied for a rectangular wing of $\mathcal{R} = 8$ at 5-deg angle of attack as shown in Fig. 5, where the number of panels in the spanwise direction is varied from $Ny = 6$-18. The wake geometry is usually converged after three iterations. Such rapid convergence is attributed to two factors: the robust scheme in the first iteration, and the use of cosine spacing for the panel distribution in the spanwise direction. It is seen that the nodes of the converged wake shapes at 1.69 span lengths behind the TE virtually fall on top of one another and form a defined contour which is predicted consistently by the present method. It is also learned that as the number of the spanwise panels increases (bringing the outboard panel closer to the tip) the wake sheet becomes more flexible and tends to roll up more. Due to the lack of vortex core modeling, however, the present method is limited to calculations with less than one turn of rollup. For this and the following calculations, the length of the near wake is taken to be two spans. For this choice and the choice of Ny, no streamwise stations of the near wake exhibit more than one turn of rollup.

A comparison with the results of Suciu and Morino[6] for a rectangular wing of $\mathcal{R} = 8$ is presented to demonstrate the validity of the method in predicting the wake rollup. The results of the converged wake shapes are shown in Fig. 6 for two different angles of attack, $\alpha = 5$ and 10 deg. In Ref. 6, the results are given at 5 chord lengths downstream of the TE. Since cosine spacing is used in the present calculation, the closest station for comparison is at 4.69. The agreement is satisfactory in the sense that Suciu and Morino use constant doublet panels to model the wake; this is equivalent to using vortex filaments. Suciu and Morino's results for the location of the vortex centers appear to agree well with the experimental observations of Chigier and Corsiglia.[14]

To illustrate the evolution of the rolled up wake pattern in the streamwise direction, Fig. 7 shows the rolled up wake sheet for a rectangular wing of $\mathcal{R} = 8$ at 5 deg angle of attack for four different downstream stations, $x_w = 0.38$, 0.82, 1.38,

and 1.69 span lengths measured from the TE with the panel arrangement of $Nx=10$ and $Ny=12$. By looking at these four streamwise stations, stretching and spiral motions are observed on the wake panels over the tip region during the rollup process while the wake sheet remains relatively flat at the middle of the wing.

In Fig. 8, a similar calculation is made for an elliptic wing of $\mathcal{R}=8$ at 5 deg angle of attack. The wake geometry is then compared with the rectangular-wing case shown in Fig. 7. Equation (9) states that the strength of the shed vorticity is proportional to the rate of change of the spanwise circulation distribution, and lifting-line theory shows that the circulation distribution depends on the local chord length. Therefore, the strength of the vorticity distribution near the tips of a rectangular wing is stronger than that of the elliptic wing of the same aspect ratio. As was expected, the wake geometry of the elliptic wing has a smaller disturbance (downward displacement) at the tips than in the rectangular-wing case.

Wing-Flap Configuration

The capability of the present method to predict the multiple rollup of the wake behind a rectangular wing with a deflected flap is also studied herein. The flap is located at the central part of the wing and has the dimensions of $b_f=b/2$ and $c_f=c/4$, where b_f and c_f are the flap span and chord, respectively. The spanwise circulation distribution of the wing-flap configuration is found numerically by using lifting-line theory where the angle of incidence $\alpha(y)$ becomes a function of the spanwise location,

$$\alpha(y)=\alpha_a, \qquad 0<y\leq b_f/2 \tag{20}$$

$$\alpha(y)=\alpha, \qquad b_f/2<y<b/2 \tag{21}$$

where α_a is the absolute angle of attack and can be obtained from thin-airfoil theory[12] by treating the flap section as a two-dimensional cambered airfoil.

Figure 9 shows the circulation distribution curves for a rectangular wing of $\mathcal{R}=8$ at $\alpha=5$ deg with the flap deflection angles $\delta_f=0$, 2, and 5 deg. It is noted that the rate of change of circulation at the flap-tip region increases as the flap deflection angle becomes large. As a result of the partial-flap configuration, the use of cosine spacing for the panel distribution in the spanwise direction is modified. Instead of putting all of the emphasis on the wingtip, equal $\Delta\Gamma$ spacing is employed for the inboard portion ($\sim 80\%$ of the span) while the cosine-spaced panels at the wingtip ($\sim 20\%$ of the span) are still being used.

Figure 10 presents the rolled up wake geometry at two downstream stations, $x_w/b=0.59$, 1.69 for a rectangular wing of $\mathcal{R}=8$ at $\alpha=5$ deg and $\delta_f=2$ deg. Similar results are also presented in Fig. 11 for $\delta_f=5$ deg. A wide range of combinations of the panel spacing was used, but only the three successful results are shown. When the chosen spacing allows for the rollup of both the flap and tip vortices, the same basic sheet shape is predicted. The main cause of the unsuccessful numerical experimentations starts from the internal rollup of the flap vortex. It is seen that the continuous vortex sheet tends to break apart when the amount of the flap-vortex rollup tightens as a result of a fine spanwise mesh in the neighborhood of the flap-tip region. On the other hand, a coarse spanwise mesh tends to smear out the effects of the deflected flap, which may not give the correct vorticity distribution. Therefore, it is thought that vortex core modeling at the flap tip, as shown in Fig. 12, may be a possible cure for the unstable wake rollup calculations of the wing-flap configuration. This approach is taken in Hoeijmakers[1] in conjunction with a two-dimensional unsteady calculation. It is also interesting to note that the additional amount of rollup for the flap vortex results in a smaller rollup at the wingtip as shown in Fig. 10.

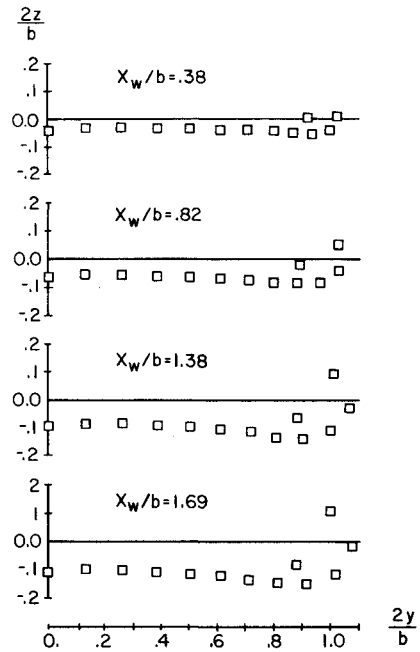

Fig. 7 Wake geometry at different downstream stations for a rectangular wing: $\mathcal{R}=8$; $\alpha=5$ deg.

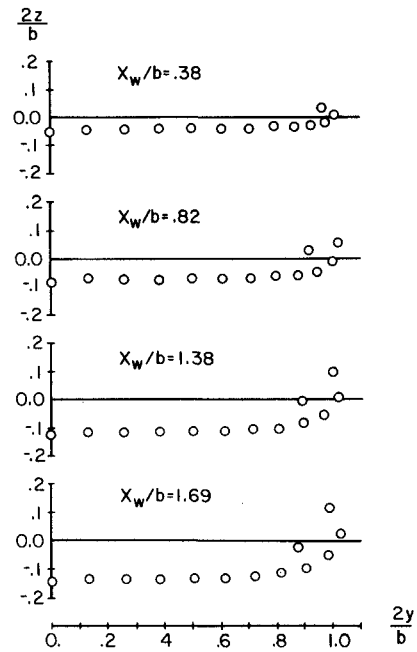

Fig. 8 Wake geometry at different downstream stations for an elliptic wing: $\mathcal{R}=8$; $\alpha=5$ deg.

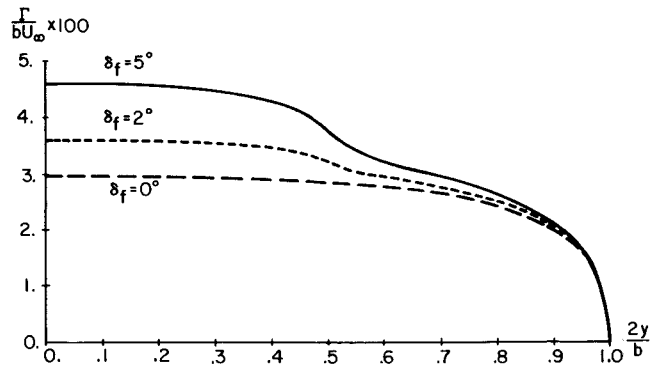

Fig. 9 Spanwise circulation distribution for a rectangular wing-flap model of $\mathcal{R}=8$ at $\alpha=5$ deg with flap deflection angles of $\delta_f=0$, 2, and 5 deg.

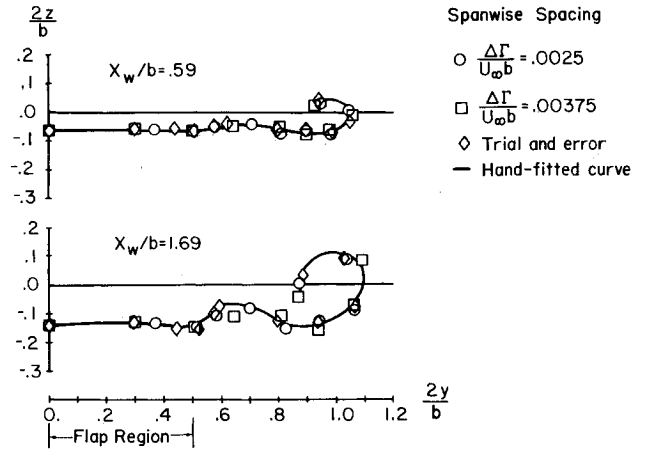

Fig. 10 Wake rollup for a rectangular wing-flap model: $\mathcal{R}=8$; $\alpha=5$ deg; $\delta_f=2$ deg, at two streamwise stations.

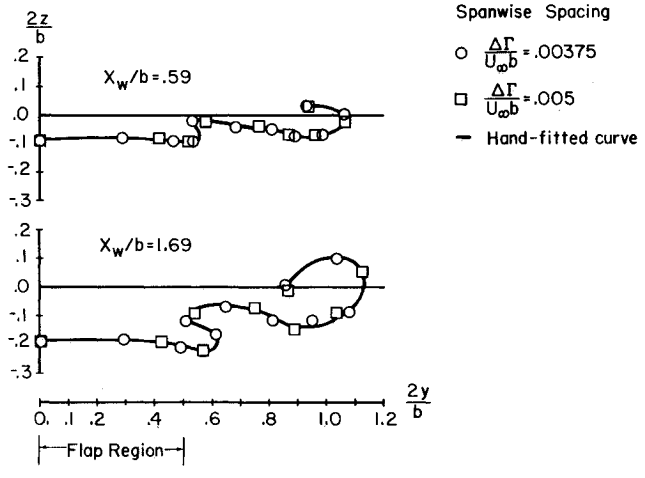

Fig. 11 Wake rollup for a rectangular wing-flap model: $\mathcal{R}=8$; $\alpha=5$ deg; $\delta_f=5$ deg, at two streamwise stations.

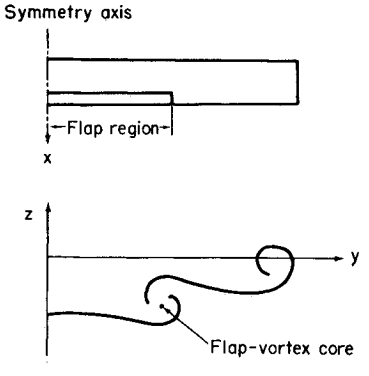

Fig. 12 Schematic view of suggested vortex core modeling.

Conclusions and Recommendations

An analysis of a higher-order (linear-vortex) panel method has been developed to calculate the wake rollup for a steady flow past a high aspect ratio wing. The present wake model bears no small-perturbation assumptions, and all of the equations engaged in the wake calculation are solved analytically. The flowfield considered here is incompressible and inviscid, and the wake is made up of triangular vortex panels in the near region and semi-infinite vortex filaments in the far region. Moreover, the method is capable of calculating the wake geometry for a variety of planforms and shapes when the spanwise circulation distribution is known either from numerical calculation or experiment (lifting-line theory is currently used).

Good comparisons are obtained between the present theory and those in the literature for the rolled up wake geometries. In addition, the capability of the method to model a wing-flap configuration is also studied. It is discovered that care is needed in the choice of the spanwise panel spacing to adequately model the regions of rapid change in wake shape.

Finally, two recommendations are suggested for further study or expansion of the method.

1) The wing as well as the wake should be modeled with linear-vortex panels to remove the restrictions on wing geometry and to provide for a more accurate modeling of the wake adjacent to the trailing edge.

2) Vortex core modeling should be included to allow for more accurate prediction of wakes with multiple rollup.

Acknowledgments

This research was supported by the Army Research Office as part of a contract to the Center for Rotorcraft Education and Research of the University of Maryland. The authors acknowledge the interest and guidance provided by Professor O. Kandil of Old Dominion University and Dr. E.C. Yates of NASA Langley. The authors also thank the Computer Science Center of the University of Maryland for supplying computer time.

References

[1]Hoeijmakers, H.W.M., "Computational Vortex Flow Aerodynamics," AGARD CP 342, 1983.

[2]Fink, P.T. and Soh, W.K., "A New Approach to Roll-Up Calculations of Vortex Sheets," *Proceedings of the Royal Society*, London, Ser. A, Vol. 362, 1978, pp. 195-209.

[3]Murman, E.M. and Stremel, P.M., "A Vortex Wake Capturing Method for Potential Flow Calculations," AIAA Paper 82-0947, 1982.

[4]Hoeijmakers, H.W.M. and Vaatstra, W., "A Higher-Order Panel Method Applied to Vortex Sheet Rollup," *AIAA Journal*, Vol. 21, April 1983, pp. 516-523.

[5]Rom, J. and Zorea, C., "The Calculation of the Lift Distribution and the Near Vortex Wake Behind High and Low Aspect Ratio Wings in Subsonic Flow," Technion-Israel Institute of Technology, Haifa, TAE Rept. 168, 1973.

[6]Suciu, E.O. and Morino, L., "A Nonlinear Finite Element Analysis of Wings in Steady Incompressible Flows with Wake Rollup," AIAA Paper 76-64, 1976.

[7]Summa, J.M., "Advanced Rotor Analysis Method for the Aerodynamics of Vortex/Blade Interactions in Hover," Eighth European Rotorcraft Forum, Paper 28, France, 1982.

[8]Morino, L., Kaprielian, Z., and Sipcic, S.R., "Free Wake Analysis of Helicopter Rotors," Ninth European Rotorcraft Forum, Paper 3, Italy, 1983.

[9]Johnson, F.T., Tinoco, E.N., Lu, P., and Epton, M.A., "Three-Dimensional Flow Over Wings with Leading-Edge Vortex Separation," *AIAA Journal*, Vol. 18, April 1980, pp. 367-380.

[10]Kandil, O.A., Chu, L., and Yates, E.C., "Hybrid Vortex Method for Lifting Surfaces with Free Vortex Flow," AIAA Paper 80-0070, 1980.

[11]Kandil, O.A., Chu, L., and Tureaud, T., "A Nonlinear Hybrid Vortex Method for Wings at Large Angles of Attack," *AIAA Journal*, Vol. 22, March 1984, pp. 329-336.

[12]Karamcheti, K., *Principles of Ideal-Fluid Aerodynamics*, John Wiley & Sons, New York, 1966.

[13]Yeh, D.T., "Vortex Panel Calculation of Wake Rollup Behind a Large Aspect Ratio Wing," M.S. Thesis, Department of Aerospace Engineering, University of Maryland, College Park, April 1985.

[14]Chigier, N.A. and Corsiglia, V.R., "Wind-Tunnel Studies of Wing Wake Turbulence," *Journal of Aircraft*, Vol. 9, Dec. 1972, pp. 820-825.